XLI CILAMCE
XLI Ibero-Latin American Congress on Computational Methods in Engineering
16-19 November, 2020 FOZ DO IGUAÇU PARANÁ - BRAZIL

A study of time integration methods for 3D FEM solution of incompressible fluids governed by the Navier-Stokes equations

André S. Müller[1], Henrique C. Gomes[1], Eduardo M. B. Campello[1]

[1]*Dept. of Structural and Geotechnical Engineering, Polytechnic School, University of São Paulo*
Av. Prof. Almeida Prado, Lane 3, 380, 05508-010, São Paulo/SP, Brazil
andre.muller@ifma.edu.br, henrique.campelo@usp.br, campello@usp.br

Abstract. This work investigates the influence of using different time integration methods for the mixed finite element formulation of tridimensional unsteady incompressible fluid flow problems governed by the Navier-Stokes equations. A classical Eulerian approach is followed to describe the fluid. A Newton-Raphson scheme is devised to solve the resulting non-linear equations within every time step of the time integration. In order to ascertain the accuracy and efficiency of the adopted methods, numerical simulations of tridimensional unsteady flow of an incompressible fluid around a cylinder are analyzed and compared against benchmark solutions.

Keywords: time integration, Navier-Stokes equations, finite element method, 3D incompressible fluid flows.

1 Introduction

Simulating the behavior of fluid flow is one of the greatest challenges for researchers in the field of Computational Fluid Dynamics (CFD). The difficulties are numerous, ranging from numerical instabilities (due e.g. to the LBB compatibility condition or the convective non-linear term) to expensive run-time consuming processes (due to the iterative solution of large systems of equations), to mention just a few. Much effort has been devoted to overcome these difficulties in the past decades (see e.g. Brooks and Hughes [1], Hughes and Franca [2], Donea and Huerta [3], Gelhart, et al. [4], Brezzi and Fortin [5], Taylor and Hood [6], Tezduyar and Osawa [7]). When it comes to unsteady three-dimensional problems, however, even in the laminar case, the simulation is still a very challenging task (Bayraktar, Mierka and Turek [8]).

In this work, the focus is to assess the performance of some of the existing time integration methods when applied to the modeling of tridimensional unsteady incompressible fluid flow problems. In particular, we aim to investigate two implicit schemes, namely, (i) the backward Euler and (ii) the Newmark [9]. Irrespective of the time integration, in all cases spatial discretization is achieved by adopting a mixed finite element formulation within a standard Galerkin framework. We use higher order tetrahedral and hexahedral finite elements with quadratic and linear shape functions to interpolate the velocity and pressure fields, respectively, which satisfies the LBB-condition (see e.g. Wieners [10], Burman and Fernández [11]). Our model is based on an Eulerian description, which allows us to avoid re-meshing or mesh adaptation during the course of the solution. Flows with low to moderate Reynolds numbers are considered in our simulations, in order to overcome possible numerical instabilities that may arise in convective-dominated problems. The non-linearity of the formulation is handled through a fully consistent Newton-Raphson scheme wherein full quadratic convergence is ensured.

We emphasize that this work is still in progress and the report presented in this article are only our partial results. We are currently implementing the other time integration methods (e.g. generalized-α method), as done by Dettmer and Peric [12]. Our aim, in a next step towards the simulation of more complex 3D fluid flows, including convection-dominated problems, is to stick to the method which showcases the best compromise between performance and accuracy in the context of three-dimensional transient flows.

2 Fluid equations

The conservation of linear momentum of an infinitesimal fluid particle of mass dm for incompressible viscous flows governed by the Navier-Stokes equations is given by

$$\rho \frac{d\boldsymbol{u}}{dt} = \text{div}\,\boldsymbol{T} + \rho \boldsymbol{b}, \tag{1}$$

where ρ, $\boldsymbol{u}$, $\boldsymbol{T}$ and $\boldsymbol{b}$ are the fluid´s mass density, velocity, Cauchy stress tensor and volumetric force per unit mass, respectively. For incompressible fluids, the mass conservation principle leads to

$$\text{div}\ \boldsymbol{u} = 0. \tag{2}$$

Considering a Newtonian fluid and an Eulerian description of the flow, the differential equations can be expressed as

$$\begin{aligned} &\boldsymbol{u} + \big(\nabla \boldsymbol{u}\big)\boldsymbol{u} - 2\nu \text{div}\Big(\nabla^S \boldsymbol{u}\Big) + \nabla p = \boldsymbol{b} \quad \text{in } \Omega, \\ &\text{div}\ \boldsymbol{u} = 0 \quad \text{in } \Omega, \end{aligned} \tag{3}$$

where ν is the fluid´s kinematic viscosity,

$$\nabla^S \boldsymbol{u} = \frac{1}{2}\Big[\nabla \boldsymbol{u} + \big(\nabla \boldsymbol{u}\big)^T\Big] \tag{4}$$

is the strain rate tensor, p is the fluid´s kinematic pressure and Ω is the flow´s domain. In order to have equation (3) well-posed, it is necessary to impose the boundary and initial conditions as follows

$$\begin{aligned} &\boldsymbol{T}\boldsymbol{n} = \overline{\boldsymbol{t}} \quad \text{in } \Gamma_t \\ &\boldsymbol{u} = \overline{\boldsymbol{u}} \quad \text{in } \Gamma_u \\ &\boldsymbol{u} = \boldsymbol{u}_0 \quad \text{in } \Omega \text{ and } t = 0, \end{aligned} \tag{5}$$

where $\boldsymbol{n}$ is the unit outward normal vector to the boundary, $\overline{\boldsymbol{t}}$ and $\overline{\boldsymbol{u}}$ are the prescribed traction and velocity vectors, respectively, and $\boldsymbol{u}_0$ is the initial velocity. The weak form of the Eq. (3) is given by

$$\big(\boldsymbol{w}, \boldsymbol{u}\big)_\Omega + c\big(\boldsymbol{u}; \boldsymbol{w}, \boldsymbol{u}\big)_\Omega + a\big(\boldsymbol{w}, \boldsymbol{u}\big)_\Omega - \big(\text{div}\boldsymbol{w}, p\big)_\Omega + \big(q, \text{div}\boldsymbol{u}\big)_\Omega - \big(\boldsymbol{w}, \overline{\boldsymbol{t}}\big)_{\Gamma_t} = \big(\boldsymbol{w}, \boldsymbol{b}\big)_\Omega \ \ \forall \boldsymbol{w}, q, \tag{6}$$

where $\boldsymbol{w}$ and q are arbitrary test functions for the velocity and pressure fields, respectively. In (6), the notation $\big(\cdot,\cdot\big)_\Omega$ means integral of the dot product of the corresponding variables over the flow domain, whereas

$$c\big(\boldsymbol{u}; \boldsymbol{w}, \boldsymbol{u}\big)_\Omega = \int_\Omega \boldsymbol{w} \cdot \big(\nabla \boldsymbol{u}\big)\boldsymbol{u} d\Omega \quad \text{and} \quad a\big(\boldsymbol{w}, \boldsymbol{u}\big)_\Omega = \int_\Omega \nabla \boldsymbol{w} : \nu \nabla \boldsymbol{u} d\Omega \tag{7}$$

are trilinear and bilinear forms of the convective and viscous terms, respectively. The boundary term over Γ_u vanishes due the fact that $\boldsymbol{w} = \boldsymbol{0}$ along Γ.

3 Time discretization and temporal integration scheme

There are several numerical methods which can be used to discretize and integrate eq. (6) in time. See, for instance, Dettmer and Peric [12], where the authors promote an extensive discussion and comparison of several time integration algorithms. In the present work, which is in its first stages as said in the introduction, we will briefly outline the Newmark [9] and backward Euler schemes next. These methods were implemented in our (in-house) code and its performance is verified through a numerical example in section 5.

3.1 Newmark and Backward Euler Method

In temporal discretizations, the time variable is discretized into time instants t^n, separated by intervals Δt, such that $t^{n+1} = t^n + \Delta t$ is the time instant immediately after t^n. In the Newmark [9] method, the acceleration of the fluid at time t^{n+1} can be expressed as

$$\boldsymbol{u}^{n+1} = \frac{1}{\gamma}\frac{\left(\boldsymbol{u}^{n+1} - \boldsymbol{u}^{n}\right)}{\Delta t} - \frac{\left(1-\gamma\right)}{\gamma}\boldsymbol{u}^{n}, \tag{8}$$

where γ is the Newmark´s integration parameter, and where superscript notation is adopted to denote the time instant at which the corresponding variable is referred to. Here, we use $\gamma = 1/2$ in order to archive second-order accuracy in the integration. Introducing eq. (8) into eq. (6) we arrive at the time-discrete weak form as follows

$$\begin{aligned}&\Big\{\big(\boldsymbol{w},\boldsymbol{u}\big)_{\Omega} + \gamma\Delta t\Big[c\big(\boldsymbol{u};\boldsymbol{w},\boldsymbol{u}\big)_{\Omega} + a\big(\boldsymbol{w},\boldsymbol{u}\big)_{\Omega} - \big(\mathrm{div}\boldsymbol{w},p\big)_{\Omega} + \big(q,\mathrm{div}\boldsymbol{u}\big)_{\Omega}\\ &-\big(\boldsymbol{w},\boldsymbol{b}\big)_{\Omega} - \big(\boldsymbol{w},\overline{\boldsymbol{t}}\big)_{\Gamma_t}\Big]\Big\}^{n+1} = \big(\boldsymbol{w},\boldsymbol{u}^{n}\big)_{\Omega} + \big(1-\gamma\big)\Delta t\big(\boldsymbol{w},\boldsymbol{u}^{n}\big)_{\Omega} \quad \forall \boldsymbol{w},q.\end{aligned} \tag{9}$$

Note that if we use $\gamma = 1$ in eq. (8), we obtain

$$\boldsymbol{u}^{n+1} = \frac{\left(\boldsymbol{u}^{n+1} - \boldsymbol{u}^{n}\right)}{\Delta t}, \tag{10}$$

which is exactly the backward Euler scheme. Then, the time-discrete weak form of eq. (6) for backward Euler is

$$\begin{aligned}&\Big\{\big(\boldsymbol{w},\boldsymbol{u}\big)_{\Omega} + \Delta t\Big[c\big(\boldsymbol{u};\boldsymbol{w},\boldsymbol{u}\big)_{\Omega} + a\big(\boldsymbol{w},\boldsymbol{u}\big)_{\Omega} - \big(\mathrm{div}\boldsymbol{w},p\big)_{\Omega} + \big(q,\mathrm{div}\boldsymbol{u}\big)_{\Omega}\\ &-\big(\boldsymbol{w},\boldsymbol{b}\big)_{\Omega} - \big(\boldsymbol{w},\overline{\boldsymbol{t}}\big)_{\Gamma_t}\Big]\Big\}^{n+1} = \big(\boldsymbol{w},\boldsymbol{u}^{n}\big)_{\Omega} \quad \forall \boldsymbol{w},q.\end{aligned} \tag{11}$$

4 Spatial discretization

We perform spatial discretization of eq. (9) by a standard mixed finite element scheme where the velocity and pressure fields are the primitive variables of the problem. The fluid domain is discretized with tetrahedral or hexahedral elements, possessing quadratic shape functions for the velocity field and linear shape functions for the pressure field. We write the finite element approximations as

$$\begin{aligned}\boldsymbol{v} &\approx \mathbf{N}_{v}\mathbf{v}_{e} \quad \text{and} \quad p \approx \mathbf{N}_{p}\mathbf{p}_{e},\\ \boldsymbol{w} &\approx \mathbf{N}_{v}\mathbf{w}_{e} \quad \text{and} \quad q \approx \mathbf{N}_{p}\mathbf{q}_{e},\end{aligned} \tag{12}$$

where $\mathbf{N}_{v}$ and $\mathbf{N}_{p}$ are matrices with the element´s shape functions of the velocity and pressure fields, respectively, and $\mathbf{v}_{e}$ and $\mathbf{p}_{e}$ are the element´s nodal values of velocity and pressure, respectively. Applying (12) into (9) we reach the algebraic matrix form of the problem as follows

$$\begin{cases}\dfrac{\mathbf{M}}{\gamma\Delta t}\mathbf{v}^{n+1} + \mathbf{C}\mathbf{v}^{n+1} + \mathbf{K}\mathbf{v}^{n+1} + \mathbf{G}\mathbf{p}^{n+1} = \mathbf{f}^{n+1} + \dfrac{\mathbf{M}}{\gamma\Delta t}\mathbf{v}^{n} + \dfrac{\left(1-\gamma\right)}{\gamma}\mathbf{M}\mathbf{v}^{n}\\ \mathbf{G}^{\mathrm{T}}\mathbf{v}^{n+1} = \boldsymbol{0}\end{cases}, \tag{13}$$

where $\mathbf{M}$, $\mathbf{C}$, $\mathbf{K}$, $\mathbf{G}$ and $\mathbf{G}^{\mathrm{T}}$ are the mass matrix, convective matrix, viscous matrix, gradient operator and divergent operator, respectively. Still in eq. (13), $\mathbf{f}^{n+1}$ is the vector of the field forces and boundary conditions. Equation (13) is non-linear due to convective term, and its solution is pursued here through a Newton-Raphson scheme wherein full quadratic convergence is warranted. For detailed information about its numerical derivation and implementation, the interested reader is referred to Gomes and Pimenta [13]. The eq. (13) can be easily rewrite for backward Euler just applying $\gamma = 1$ in it, as mentioned in section 3.

5 Numerical examples

5.1 3D Laminar flow around a cylinder

This example is a classical benchmark in the CFD community (see e.g. Schäfer and Turek [14], Bayraktar, Mierka and Turek [8], Turek and Schäfer [15]). It consists of a three-dimensional laminar flow around a cylinder

with circular cross-section within a narrow channel. The geometry and the boundary conditions are illustrated in Figure 1.

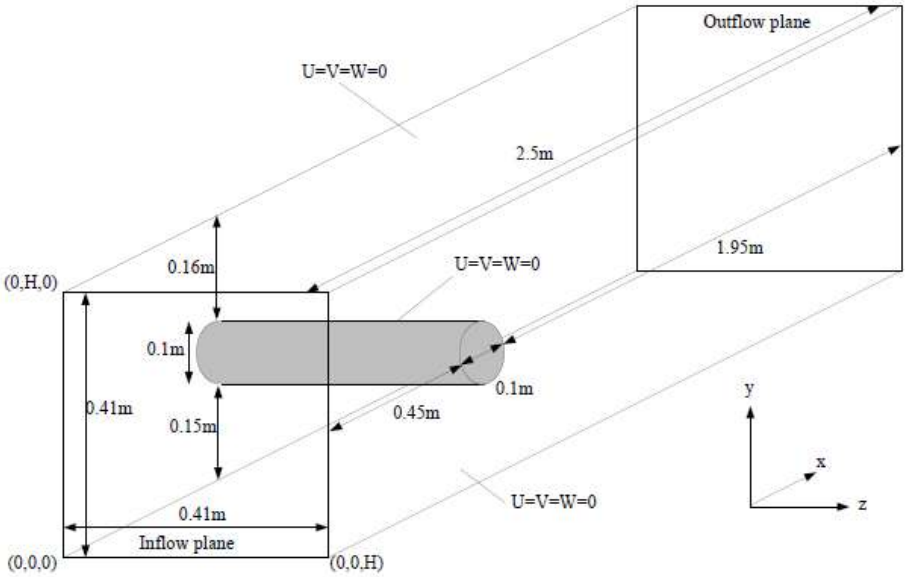

Figure 1. Geometry and boundary conditions for 3D laminar flow around a cylinder with circular cross-section (figure from Schäfer and Turek [14]).

The fluid velocity profile at the inflow section of the channel is

$$U\left(0,y,z\right)=\frac{16U_m yz\left(H-y\right)\left(H-z\right)}{H^4},\quad V=W=0 \tag{14}$$

where $U_m=2.25$ m/s and $H=0.41$ m, from which the Reynolds number is $\mathrm{Re}=100$. The kinematic viscosity is defined as $\nu=10^{-3}$ m^2/s, and the fluid density is $\rho=1.0$ kg/m^3. The time interval used in this example is $0\leq t\leq 4.0s$. Notation for the velocity components is $\left(u_1,u_2,u_3\right)=\left(U,V,W\right)$ and the boundary condition at outflow plane is zero traction. The convergence tolerance used within the Newton-Raphson iterations is $\mathrm{TOL}=10^{-6}$. Figure 2 shows the finite element mesh used herein.

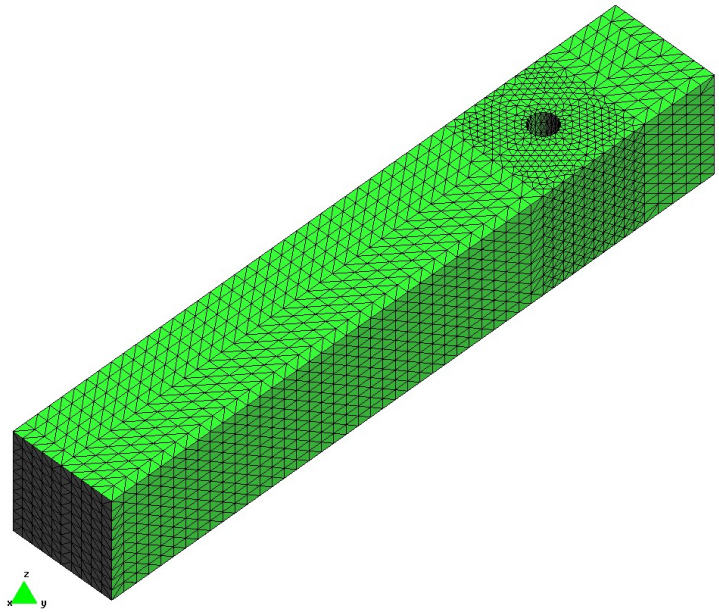

Figure 2. Finite element mesh used, 67533 tetrahedral elements and 96684 nodes.

Three different Δt were used in order to assess the convergence of the results only for Newmark [9], namely: $\Delta t = 0.01s$, $\Delta t = 0.02s$ e $\Delta t = 0.005s$. Visually there was no significant difference in results between Δt, therefore, Figure 3 shows some results in velocity and pressure fields for a qualitative assessment of the results only for $\Delta t = 0.01s$. Hotter colors indicate higher values.

Results for Δt = 0.01s – Newmark scheme

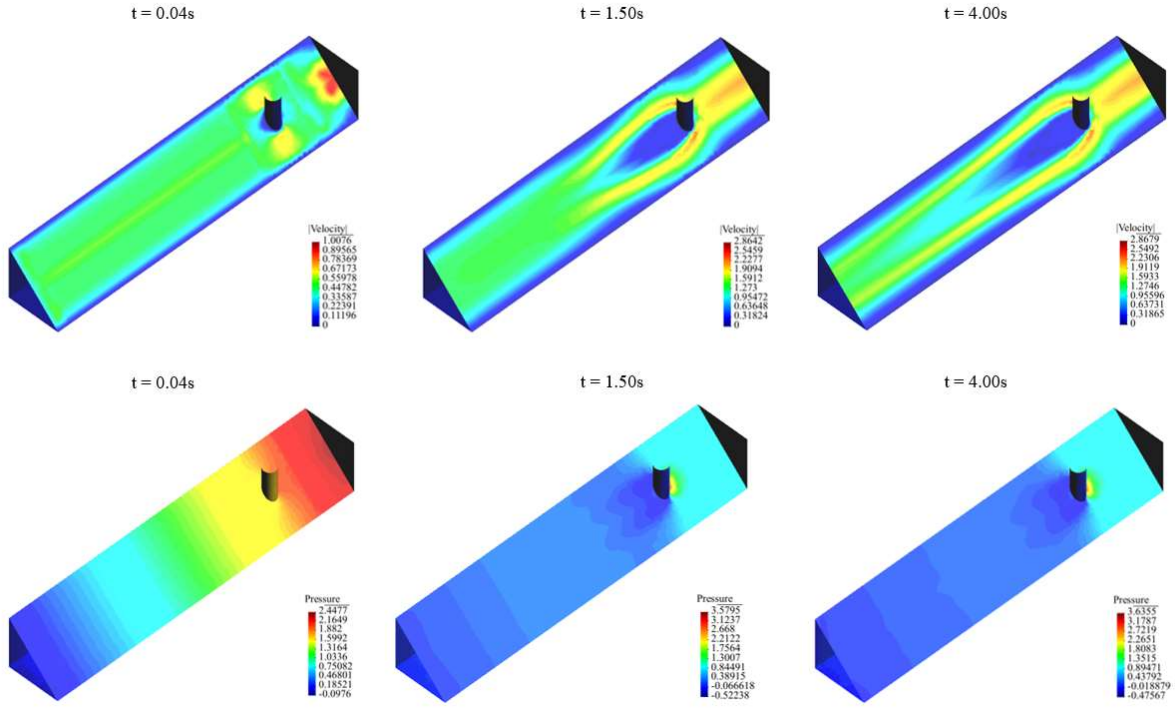

Figure 3. Velocity and pressure fields for Re = 100 (Δt = 0.01s).

For a quantitative assessment, the evolution in time of pressure difference (ΔP), the drag (Cd) and lift (Cl) coefficients were evaluated applying Newmark [9] and backward Euler schemes for $\Delta t = 0.005s$. We used a refined mesh only around the cylinder using hexahedral elements as shown in Figure 4 to reach better results.

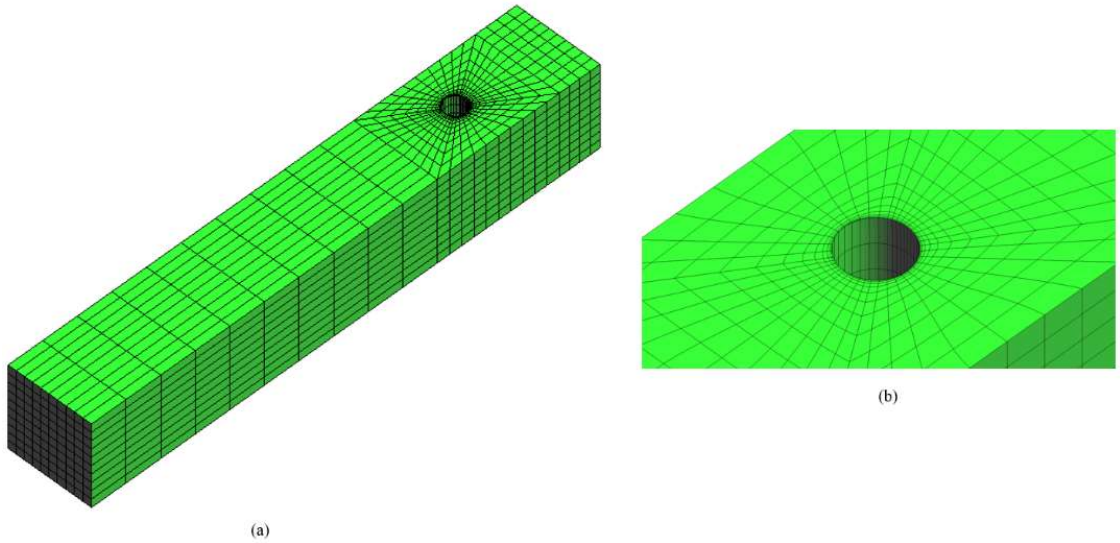

Figure 4. (a) - Finite element mesh used to evaluate ΔP , Cd and Cl coefficients (6200 hexahedral elements and 54348 nodes); (b) - Detail of the mesh around the cylinder.

The pressure difference was evaluated at the points $\Delta P(t) = P(0.45, 0.20, 0.205) - P(0.55, 0.20, 0.205)$. The results for pressure difference are shown in Figure 5.

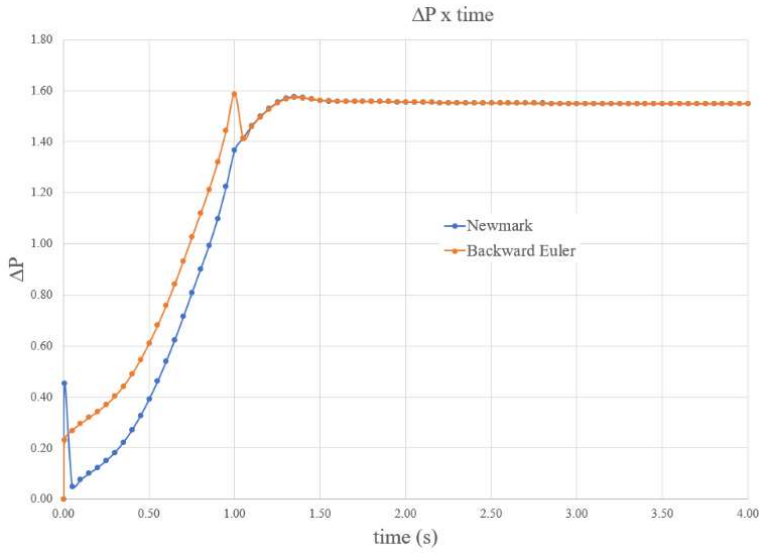

Figure 5. Graphic of ΔP for Newmark [9] and backward Euler schemes.

The results for Cd and Cl coefficients are shown in Figure 6. After the problem stabilization, these results were compared with Schäfer and Turek [14] as we can see in Table 1.

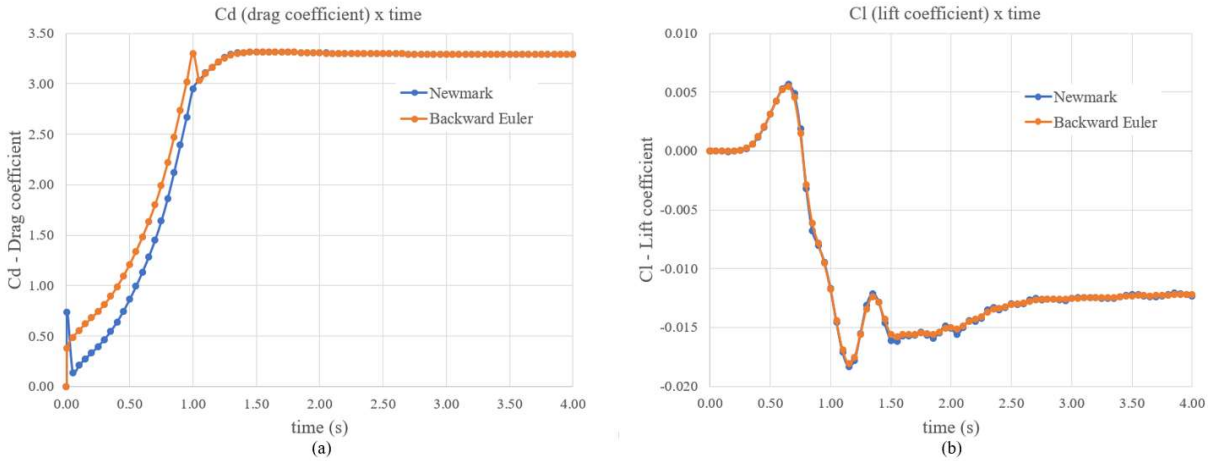

Figure 6. (a) - Graphic of Cd x time; (b) - Graphic of Cl x time.

Table 1. Cd and Cl coefficients.

Integration scheme		Cl	Cd
Newmark		-0.0123	3.2933
Backward Euler		-0.0122	3.2933
Schäfer and Turek [14]	lower bound	-0.0110	3.2900
	upper bound	-0.0080	3.3100

6 Conclusions

This work presented our first result for 3D unsteady fluid flow governed by Navier-Stokes equations. As we already mentioned, this works is still in progress and we plan to investigate other aspects that may influence the results, for instance, the effect of the mesh refinement around the cylinder and other time integration scheme (e.g. generalized-α method). As concerned only to the Newmark [9] scheme, the results shown a good convergence between chosen Δt (see Figure 3). After the problem stabilization, the results regarding the ΔP , Cd and Cl coefficients for Newmark [9] and backward Euler schemes also shown good agreement (see Figure 5, Figure 6 and Table 1). Of course, we still have work to do but we understand that our result show that we are at the right direction.

Acknowledgements. The first author acknowledges support by Federal Institute of Maranhão, Brazil, and its Department of Civil Construction, also acknowledges scholarship funding from FAPEMA (Fundação de Amparo à Pesquisa e ao Desenvolvimento Científico e Tecnológico do Maranhão) under the grant BD-02045/19. Third author acknowledges support by CNPq (Conselho Nacional de Desenvolvimento Científico e Tecnológico), Brazil, under the grants 309748/2015-1 and 307368/2018-1.

Authorship statement. The authors hereby confirm that they are the sole liable persons responsible for the authorship of this work, and that all material that has been herein included as part of the present paper is either the property (and authorship) of the authors, or has the permission of the owners to be included here.

References

[1] A. N. Brooks e T. J. R. Hughes, "Streamline upwind/petrov-galerkin formulations for convective dominated flows with particular emphasis on the incompressible Navier-Stokes equations," *Computer Methods in Applied Mechanics and Engineering,* vol. 32, pp. 199-259, 1982.

[2] T. J. R. Hughes e L. P. Franca, "A new finite element formulation for computational fluid dynamics: VII. The Stokes problem with various well-posed boundary conditions: symmetric formulations that converge for all velocity/pressure spaces," *Comput. Methods Appl. Mech. Engrg,* pp. 85-96, 1987.

[3] J. Donea e A. Huerta, The finite element method for flow problems, John Wiley, 2003.

[4] T. Gelhard, G. Lube, M. Olshanskii e J. Starcke, "Stabilized finite element schemes with LBB-stable elements for incompressible flows," *Journal of Comp. and Applied Mathematics,* pp. 243-267, 2005.

[5] F. Brezzi e M. Fortin, "Mixed and hibrid finite element methods," *Springer-Verlag New York,* 1991.

[6] C. Taylor and P. Hood, "A numerical solution of the Navier-Stokes equations using the finite element technique," *Computers & Fluids,* pp. 73-100, 1973.

[7] T. E. Tezduyar and Y. Osawa, "Finite element stabilization parameters computed from element matrices and vectors," *Computer Methods in Applied Mechanics and Engineering,* pp. 411-430, 2000.

[8] E. Bayraktar, O. Mierka e S. Turek, "Benchmark computations of 3D laminar flow around a cylinder with CFX, OpenFOAM and FeatFlow," *International Journal of Comp. Science and Eng.,* pp. 253-266, 2012.

[9] N. M. Newmark, "A method of computation for structural dynamics," *Journal of the Engineering Mechanics Division,* pp. 67-94, Julho 1959.

[10] C. Wieners, Taylor-Hood elements in 3D. In: Wendland, W.; Efendiev, M. (eds) Analysis and simulation of multifield problems. Lecture Notes in Applied and Computational Mechanics, Berlin: Springer, 2003.

[11] E. Burman e M. A. Fernández, "Stabilized finite element schemes for incompressible flow using velocity/pressure spaces satisfying the LBB-condition," em *Proceedings of the WCCM VI*, Beijing, 2004.

[12] W. Dettmer and D. Peric, "An analysis of the time integration algorithms for the finite element solutions of incompressible Navier-Stokes equations based on a stabilised formulation," *Computer methods in applied mechanics and engineering,* pp. 1177-1226, 2002.

[13] H. C. Gomes e P. M. Pimenta, "Embedded Interface with Discontinuous Lagrange Multipliers for Fluid-Structure Interaction Analysis," *International Journal for Computational Methods in Engineering Science and Mechanics,* pp. 98-111, 24 04 2015.

[14] M. Schäfer e S. Turek, "Benchmark computations of laminar flow around a cylinder," *Numer. Fluid Mech.,* pp. 547-566, 1996.

[15] S. Turek e M. Schäfer, "Recent benchmark computations of laminar flow around a cylinder," *Proceedings of the 3rd World Conference in Applied Computational Fluid Mechanics,* 1996.